

ОБЪЕДИНЕННЫЙ
ИНСТИТУТ
ЯДЕРНЫХ
ИССЛЕДОВАНИЙ
ДУБНА

E 43

E1-87-547

**FRAGMENTATION OF ^{22}Ne
IN EMULSION AT 4.1 A GeV/c**

Collaboration

Submitted to "Journal of Physics G
(Nuclear Physics)"

1987

A.El-Naghy, S.A.Krasnov, K.D.Tolstov
Joint Institute for Nuclear Research, Dubna

N.P.Andreeva, Z.V.Anzon, V.I.Bubnov, I.Ya.Chasnikov,
G.Zh.Eligmaeva, L.E.Eremenko, A.Sh.Gaitinov, G.S.Kalyachkina,
E.K.Kanygina, Ts.I.Shakhova
Institute of High Energy Physics, Alma-Ata, USSR

M.Gitsok, M.Haiduc, V.Topor
Central Institute of Physics, Bucharest, Romania

V.A.Leskin
Physical Technical Institute of Dushanbe, USSR

J.A.Salomov
Tadjik State University, Dushanbe, USSR

F.G.Lepekhin, B.B.Simonov
Leningrad Nuclear Physical Institute, Gatchina, USSR

M.Karabova, M.Totrova, S.Vokal, E.Siles
Safarik University, Kosice, Czechoslovakia

V.A.Antonchik, S.G.Bogdanov, A.Y.Likhachev, V.I.Ostroumov
Leningrad Polytechnic Institute, Leningrad, USSR

V.G.Bogdanov, V.A.Plyushchev, Z.I.Solovieva
V.G.Khlopin Radium Institute, Leningrad, USSR

M.I.Adamovich, M.M.Chernyavski, S.P.Kharlamov, V.G.Larionova,
N.V.Maslennikova, G.I.Orlova, N.A.Salmanova, M.I.Tretyakova
P.N.Lebedev Physical Institute, Moscow, USSR

A.V.Belousov
Azovo-Chernomorski Institute of Agriculture Mechanization,
Rostov on Don, USSR

M.Sumbera
Nuclear Physics Institute, Rež, Czechoslovakia

N.I.Kostanashvili
Tbilisi State University, Tbilisi, USSR

L.Sardamba, R.Togoo, D.Tuvdendorzh
Institute of Physics and Technique, Ulan-Bator, Mongolia

F.A.Avetyan, V.M.Krishchyan, M.A.Marutyan, L.G.Sarkisova,
V.R.Sarkisyan
Yerevan Physical Institute, Yerevan, USSR

1. Introduction

In nucleus-nucleus collisions, the nucleons in the overlap region are called participants. The remaining nucleons are spectators. Large impact parameters lead to "gentle" reactions while small ones give "violent" interactions. The spectators are the prefragments which further decay into fragments. The mechanism of this process is still a matter of debate. Fragmentation is one of the historical^{/1/} and fundamental questions^{/2-4/} in high energy nuclear physics. The author of^{/2/} schematically distinguished three main mechanisms for the fragmentation of $A \geq 200$ prefragment nucleus: the first mechanism is spallation which leads to one fragment of mass near that of the prefragment nucleus, the second one is fission which gives two heavy fragments, each of mass close to half the prefragment nucleus mass. Multifragmentation is the third mechanism which provides several fragments. In^{/3,4/} the fragmentation processes are divided according to the temperature, T , of the prefragment nucleus as follows: at $T \leq 5$ MeV the mass yield distribution is localized near the minimal and maximal masses corresponding to single nucleons and residual nuclei. At $T \approx 5-7$ MeV the mass distribution has a U-shaped form which indicates the multifragmentation threshold. At $T > 7$ the inclusive mass yield distribution becomes a monotonously decreasing function, the steepness of which increases with increasing T .

Many theoretical models have been devoted to the study of the multifragmentation process^{/2-16/}. In some models, the prefragment nucleus heats up and then condensates into droplets^{/5,6/}. In others, it simply evaporates the fragments sequentially^{/7/}.

In /8-13/, the fragments are statistically emitted from an intermediate excited nuclear system. Other statistical approaches /14-16/ try to explain the multifragmentation without any reference to thermal equilibrium, i.e. as shattering of the prefragment nucleus into many pieces. A detailed description of different multifragmentation models is given in the review articles /2-4/.

To study the mechanism of multifragmentation, a huge number of experiments has been carried out. These experiments dealt with heavy target nucleus fragmentation induced by energetic protons and ions /e.g., 17, 18/. The use of heavy ion beams has an important experimental advantage: one can study the fragments produced by the disintegration of the projectile nucleus. The fragments of the projectile nucleus are fast, distinguishable and can be easily measured in detectors and/or spectrometers while the target fragments are slow, difficult to be measured and often stop in the target material. Most of the heavy target fragmentation experiments gave one-particle inclusive measurements, e.g. the charge $d\sigma/dZ$ or mass $d\sigma/dA$ yield of the fragments. Various models predicted nearly the same form of $d\sigma/dZ$ and $d\sigma/dA$. Thus, these data turned out to be inconclusive with respect to various models.

In the present experiment all projectile fragments (PFs) were recorded, and their charges and emission angles were measured. Thus, we have exclusive data which enable one to study different types of fragment distributions, correlations and comparison with theoretical models. It is of particular interest to test whether fragments are emitted from one source at a single excitation energy.

The paper is organized so that Sect. 2 presents the experimental details. Sect. 3 provides the selection criteria for the studied events. The results and discussions are outlined in Sect. 4. Sect. 5 is devoted to the conclusions of the present study.

2. Experiment

Stacks of Br-2 nuclear emulsions were exposed to a 4.1 A GeV/c ^{22}Ne beam at the Dubna synchrophasotron. The stacks consisted of 50 or 100 pellicles having dimensions of 20 cm \times 10 cm \times 600 μm (undeveloped emulsion). The intensity of irradiation was 10^4 particles/cm², and the beam diameter was about 1 cm. Along-the-track double scanning was carried out, fast in the forward and slow in the backward direction. The scanned beam tracks were further examined by measuring the delta-electron density on each of them to exclude the tracks having charge less than the beam particle charge. The one-prong events with an emission angle of the secondary particle track less than three degrees and without visible tracks from excitation or disintegration of the target nucleus were excluded due to elastic scattering.

Along a total scanned length of 947.4 m, 9318 inelastic interactions of ^{22}Ne ions with emulsion were recorded leading to a mean free path of 10.2 ± 0.1 cm for inelastic interactions. This value and other experimental details were published by our collaboration in /19-23/. In the measured events, the secondary particles are classified as follows: (i) black particle tracks (b) having a range $L \leq 3$ mm in emulsion which corresponds to a proton kinetic energy of ≤ 26 MeV, (ii) grey particle tracks (g) having relative ionization $I^* (=I/I_0) > 1.4$ and $L > 3$ mm which corresponds to a proton kinetic energy from 26 to 400 MeV, where I is the particle track ionization and I_0 is the ionization of a shower track in the narrow forward cone of an opening angle of 3° . (iii) The b and/or g particle tracks are called heavy ionizing particle tracks (h). (iv) The shower particles s having $I^* \leq 1.4$. Tracks of such a type with an emission angle of $\leq 5^\circ$ were further subjected to rigorous multiple scattering measurement for momentum determination and, consequently, for separating the produced pions

from singly charged projectile fragments (protons, deuterons and tritons). The ratio of $^1\text{H} : ^2\text{H} : ^3\text{H}$ was found to be 63:27:10^{/23/}. Further the $Z=1$ PFs are not included in s particles.

(v) The multicharged $Z \geq 2$ PFs are subdivided into $Z=2,3, \dots, 10$ fragments according to the measured delta-electron and/or gap density. Thus, all particles were adequately divided into PFs of $Z=1 \div 10$, target fragments (TFs), i.e. h particles, and the generated s particles. The total charge of the PFs, $Z^* = \sum n_i Z_i$, was calculated in each star, where n_i is the number of fragments of charge Z_i in an event. For each track we obtained from measurements: (a) the polar angle θ , i.e. the space angle between the direction of the beam and that of the given track, (b) the azimuthal angle ϕ , i.e. the angle between the projection of the given track in the plane normal to the beam and the direction perpendicular to the beam in this plane (in an anticlockwise direction).

3. Selection Criteria

Two samples of 4.1 GeV/c ^{22}Ne -emulsion collisions have been used in the present study. The first sample consists of 4307 events measured in this experiment (EXP) and the second of 4976 events simulated in a computer by the cascade-evaporation model (CEM)^{/24/} under the same experimental conditions. From the two samples we selected events having the total charge of PFs, $Z^* = 10$, i.e. those conserving the beam charge. Thus, 855 events from the experimental sample and 553 events from the simulated interactions have been chosen for the present study. Here we study the charge yield distribution for the ^{22}Ne projectile fragmentation, the fragment-fragment correlation and the relation between PFs and TFs. This enables us to distinguish between different theoretical models.

4. Results and Discussion

The multiplicity characteristics of the events selected from EXP and CEM are presented in Table 1. The values of $\langle n_s \rangle$, $\langle n_g \rangle$, and $\langle n_b \rangle$ in CEM are systematically higher than the corresponding values in EXP. Light and heavy PFs are produced in CEM more copiously than in EXP. The PFs of medium charge $Z = 4 \div 6$ are nearly absent in CEM. This can be explained by the fact that in CEM the light fragments are produced by evaporation and the heavy ones are just residual nuclei of the prefragment systems. Table 1 demonstrates that there is a great deviation between CEM and EXP

Table 1. The multiplicity characteristics of the selected events of the total charge of PFs, $Z^* = 10$, from EXP and CEM

	EXP	CEM
$\langle n_s \rangle$	$1.30 \pm .06$	$1.91 \pm .09$
$\langle n_g \rangle$	$0.96 \pm .06$	$1.46 \pm .10$
$\langle n_b \rangle$	$1.44 \pm .07$	$2.34 \pm .13$
$\langle n_{z=i} \rangle, i = 1$	$0.99 \pm .05$	$1.59 \pm .11$
2	$0.81 \pm .04$	$0.36 \pm .04$
3	$0.02 \pm .01$	$0.00 \pm .00$
4	$0.03 \pm .01$	$0.01 \pm .01$
5	$0.04 \pm .01$	$0.01 \pm .01$
6	$0.12 \pm .01$	$0.02 \pm .01$
7	$0.15 \pm .01$	$0.02 \pm .01$
8	$0.23 \pm .02$	$0.05 \pm .01$
9	$0.10 \pm .01$	$0.12 \pm .01$
10	$0.26 \pm .02$	$0.59 \pm .02$

in all average multiplicities of fragments. Table 2 shows the catalogue of 855 selected events, i.e. those having the total charge of PFS, $Z^* = 10$. One can see different channels of fragmentation ordered according to Z_{\max} , the charge of the heaviest PF emitted in an interaction. At the beginning one can observe the "gentle" spallation process in which one or two particles are evaporated from the prefragment nucleus leaving the residual nucleus which cools down forming a heavy fragment. This process is characterized by low excitation energy and temperature. On the contrary, at the end of the table one can notice a "violent" process in which the prefragment Ne nucleus has been destroyed in-

Table 2. The catalogue of the selected events. Different channels of fragmentation are ordered according to Z_{\max} .

Fragmentation Channel	Frequency	Fragmentation Channel	Frequency
Ne	222	H + Be + B	2
H + F	82	5H + B	4
He + O	142	2B	1
2H + O	49	2H + 2He + Be	9
H + He + N	102	4H + He + Be	5
3H + N	24	3He + Be	4
2H + He + C	54	H + He + Li + Be	1
2He + C	29	3H + 2He + Li	7
4H + C	14	H + 3He + Li	4
H + Li + C	2	7H + Li	1
Be + C	1	H + 3Li	1
3H + He + B	14	5He	10
H + 2He + B	13	2H + 4He	30
		4H + 3He	14
		6H + 2He	5
		8H + He	3

to H and He fragments. Fig.1 shows the charge yield curve for fragment production from the ^{22}Ne projectile in the case of collision with emulsion. The distribution has a characteristic U-shaped form. In the region of small Z, the curve decreases, then it rises for large values of Z. The number of target fragments N_h can be used as a measure of the "violence" of a collision. To demonstrate the correlation between PFS and N_h , Fig.2 shows the charge distribution of PFS for a sub-class of events of $N_h = 1$ and $N_h = 4$. In the former case a nearly symmetric U-shaped distribution is obtained which is connected with the "gentle" low temperature process. In the latter case the distribution decreases from light to heavier fragments. The class of $N_h = 1$ events cannot be totally attributed to the "gentle" peripheral collisions. Fragments of

Fig.1. The charge yield distribution of PFS from ^{22}Ne fragmentation in emulsion at 4.1 A GeV/c.

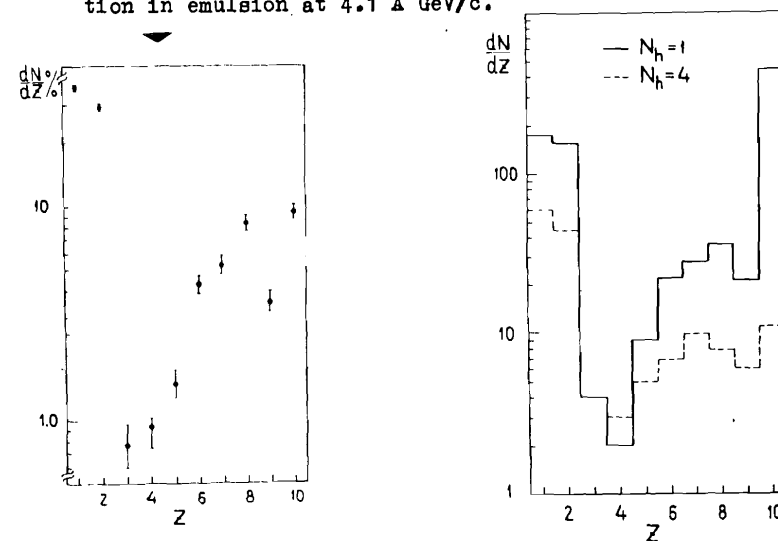


Fig.2. The charge yield distributions of PFS from $N_h = 1$ and $N_h = 4$ events.

Table 3. The charge distribution of PFs as a function of the number of singly charged PFs, N_1

N_1	0	1	2	3	4	5	6	7	8	9	10
10	222*										
9		82									
8	142		49								
7		102	24								
6	30	2	54	14							
5	2	15		14	4						
4	5	3	9		5						
3		10		7		1					
2	262	141	192	28	47	10					3
1		207	284	135	132	20	30	7	24		
Z	N_1	0	1	2	3	4	5	6	7	8	

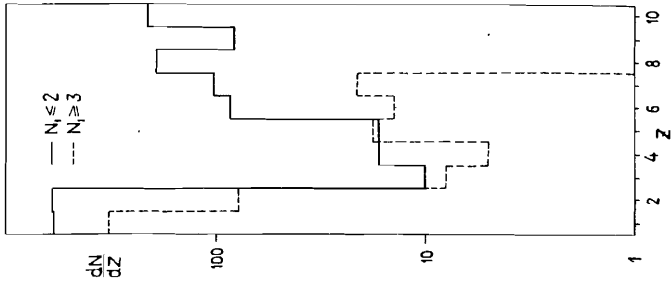


Fig.3. The charge yield distributions of PFs from events of the number of singly charged PFs, $N_1 \leq 2$ and $N_1 \geq 3$.

small Z , in this class of events, are mostly the products of "non-peripheral" collisions between ^{22}Ne and emulsion. In these events a target nucleon dives into the ^{22}Ne projectile nucleus destroying it into small fragments. The size of the largest fragment which can be formed from the projectile spectator nucleus decreases with decreasing the impact parameter. At $N_h = 1$, fragments of large Z are the evaporation residues of peripheral collisions. Thus, light fragments ($Z = 1$ and 2) are the products of either "gentle" evaporation or "violent" multifragmentation.

The degree of "violence" of a collision can be characterized by the number of singly charged projectile fragments N_1 . These fragments are from different sources: direct pickup during the intranuclear cascade, evaporation and the smallest fragments of the multifragmentation process. In any of these cases the production rate should increase with the degree of "violence" of the collision or with the excitation energy of the emitting source. Table 3 shows the charge distribution of PFs as a function of N_1 . Fig.3 shows that the charge distribution takes the U-shaped form in the case of $N_1 \leq 2$ while it decreases for $N_1 \geq 3$. This behaviour is more pronounced in the class of $N_h = 0$ events. Fig.4 displays the charge distribution for $N_1 = 0$ and $N_1 \geq 4$ events. The transition from the U-shaped distribution to the monotonously decreasing one is more obvious in this case.

Another measure of the "violence" of a collision is Z_{max} , the charge of the largest PF emitted in the interaction. Table 4 shows the dependence of the charge distribution of PFs on Z_{max} . At large values of Z_{max} , i.e. "gentle" collisions, the charge distribution of PFs is a nearly symmetric U-shaped one. At low values of Z_{max} , i.e. "violent" collisions, the charge distribution is a decreasing function. These features are seen better in Fig.5, where the charge distributions are presented for $Z_{\text{max}} \geq 6$ and

Fig.4. The charge yield distributions of PFs from $N_h = 0$ events for $N_1 = 0$ and $N_1 \geq 4$.

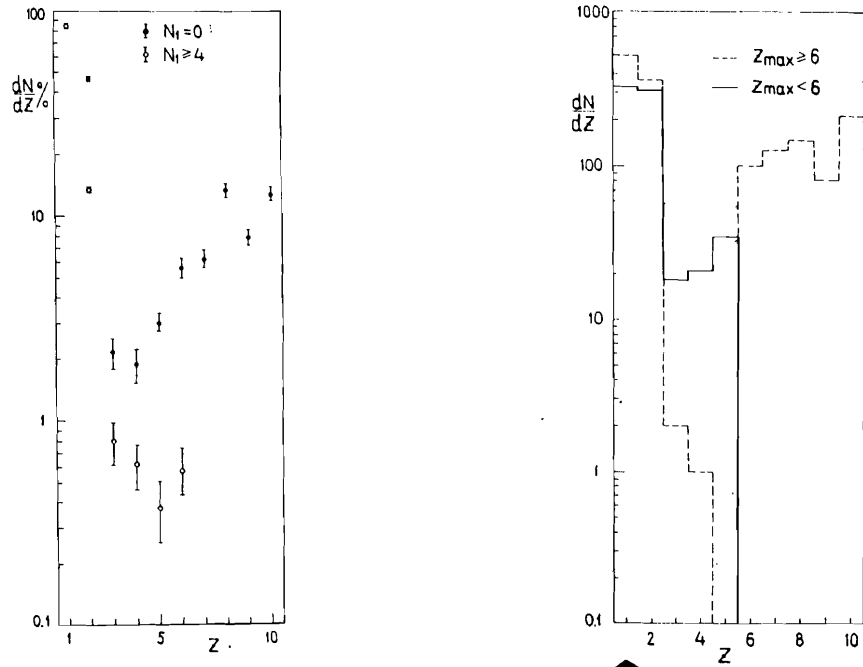


Fig.5. The charge yield distributions of PFs from events of $Z_{max} \geq 6$ and $Z_{max} < 6$.

$Z_{max} < 6$ events. The analysis of Figs. 1-5 and Tables 1-4 shows that the inclusive charge yield distribution of fragments is a superposition of different mechanisms. One can at least distinguish two main classes of mechanisms: gentle evaporation and violent multifragmentation. The authors of [17] have interpreted the mass yield curve in the frame of liquid gas transition. The present analysis shows that this claim is not conclusive; singly and doubly charged fragments are obviously due to different mechanisms.

Table 4. The dependence of the charge distribution of PFs on Z_{max}

10										222	
9	82									82	
8	98	142							191		
7	174	102				126					
6	176	112	2	1		100					
5	77	40		2	35						
4	39	36	1	19							
3	33	26	15								
2	180	225									
Z_{max}											
	2	1	2	3	4	5	6	7	8	9	10

Table 5. The $\langle n_B \rangle$ and $\langle N_h \rangle$ as a function of the number of PFs

$\langle N_{PF} \rangle$	\dot{E}^*/A	$\langle n_B \rangle$	$\langle N_h \rangle$
1.51	5	$0.64 \pm .08$	$1.94 \pm .18$
3.35	7	$1.82 \pm .15$	$2.69 \pm .31$
5.47	15	$2.44 \pm .38$	$3.19 \pm .61$
7.62	18	$2.81 \pm .97$	4.04 ± 1.38

The violence of the interaction can be measured by the multiplicities of target fragments associated with a projectile fragment. Table 5 presents $\langle n_B \rangle$ and $\langle N_h \rangle$ as a function of the number of PFs. The first column represents the average number of PFs. The second column is the excitation energy per nucleon (in MeV) of the prefragment nucleus calculated according to the statistical model⁴. The third and fourth columns represent the average multiplicities of the associated s and h particles, respectively. The correlation between the multiplicities of PFs and TFs is clearly seen from Table 5. The values of $\langle n_B \rangle$ and $\langle N_h \rangle$ increase systematically with N_{PF} .

The class of events of $N_h = 0$, i.e. those without target fragmentation, were studied in detail for ^{12}C -emulsion collisions at 4.5 A GeV/c^{/25/} and at 2.1 A GeV/c^{/26/}. It is interesting to compare the present data with these results. The production frequency of events in ^{22}Ne -Em collisions as a function of Z_{max} is shown in Fig.6 and Table 6. It should be noted that the maximum probability is for events having $Z_{max} = 2$. In the case of 4.5 A GeV/c ^{22}C -Em collisions^{/25/}, the fraction of such events is $(62 \pm 9)\%$ of all $N_h = 0$ events. For 4.1 A GeV/c ^{22}Ne -Em, the corresponding ratio is only $(24 \pm 2)\%$. This experimental fact can be interpreted by two main reasons: (i) the ^{12}C nucleus is an even-even one of total zero spin, i.e. an α -cluster nucleus. (ii) The main channel of fragmentation is a two-particle one. In the case of ^{22}Ne -Em collisions, $\text{Ne} \rightarrow \text{He} + \text{O}$ predominates, and both He and O are stable nuclei. The corresponding channel in ^{12}C -Em collisions is $^{12}\text{C} \rightarrow \text{He} + \text{Be}$, but Be is an unstable nucleus which directly decays into 2 He nuclei. In fact, the percentage of He for ^{12}C -Em collisions is $(62 \pm 9)\%$. If this percentage is divided by two, it will be nearly equal to the corresponding value of ^{22}Ne -Em collisions. Table 6 shows that the production frequency

Table 6. The production frequency in percentage of events in emulsion as a function of Z_{max} , the charge of the heaviest PF in an interaction

Z_{max} → Beam ↓	1	2	3	≥ 4
2.1 A GeV C^{12}	7 ± 2	59 ± 10	8 ± 3	26 ± 12
4.5 A GeV C^{12}	13 ± 4	62 ± 9	15 ± 4	10 ± 3
4.1 A GeV Ne^{22}	2 ± 1	24 ± 2	4 ± 1	70 ± 4

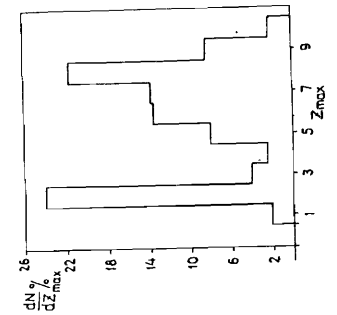


Fig.6. The production frequency of $N_h = 0$ events as a function of Z_{max} .

of events in emulsion as a function of Z_{\max} is independent of energy in the range of a few GeV/c per nucleon. It is remarkable that $Z=2$ and $Z=8$ are the first two magic numbers. This explains the peaks observed at these values in Fig.6. The results show that the nuclear structure of the prefragment nucleus plays an important role in the fragmentation process. More "gentle" fragmentations of ^{22}Ne projectile nuclei are the events of $N_h=0$ and $n_g=0$, i.e. those without target fragmentation and generation of shower particles. Table 7 presents a catalogue of the observed PFS in the 120 events of $N_h=0$ and $n_g=0$ ordered according to Z_{\max} . Out of them, the number of single- and double-prong stars is 77(64.2%). This shows a low excitation energy of the prefragment nucleus, $\epsilon_{\text{exc}/A} \approx 3\frac{1}{4} \text{ MeV}/4$.

Table 7. The catalogue of the observed PFS in events of $N_h = 0$ and $n_g = 0$ ordered according to Z_{\max}

Fragmentation Channel	Frequency
Ne	3
H + F	18
He + O	56
2H + O	8
H + He + N	10
3H + N	3
2H + He + C	3
2He + C	6
4H + C	1
He + Li + B	1
H + 2He + B	3
3 He + Be	2
2H + 2He + Be	1
2H + 4He	1
5He	4

5. Conclusions

In $^{22}\text{Ne} + \text{Em}$ collisions at 4.1 A GeV/c, events, having the total charge of PFS, Z^* , equal to the beam charge, have been selected for studying the fragmentation of ^{22}Ne in emulsion.

The inclusive charge distribution of fragments is a superposition of different mechanisms. The heavy fragments ($Z = 8-10$) as well as some of the light ones ($Z = 1,2$) originate mainly from "gentle" peripheral collisions. They show a distribution characteristic for evaporation from the compound nucleus. This process is characterized by low excitation energy. These fragments are associated with a low multiplicity of target tracks. The medium mass fragments as well as the measurable part of $Z = 1$ and 2 fragments are due to nonperipheral "violent" collisions characterized by associated large multiplicities of the target. The charge distribution of these fragments has a monotonously decreasing shape. Thus, the mechanisms claiming one hot source at a certain excitation energy for explaining the inclusive charge distribution conflict with the present analysis.

Acknowledgement

One of the authors, A. El-Naghy, would like to thank the authority of JINR for supporting him during his stay at Dubna while the present investigation was being carried out.

References

1. Perfilov N.A. et al. 1960, Usp.Fiz.Nauk, 70, 3 (in Russian).
2. Hüfner J. 1985, Phys.Rep. 125, 131.
3. Mishustin I.N. 1986, Nucl.Phys. A447, 67C.
4. Toneev V.D. et al. 1986, E.Ch.A.Ya. 17, 1093 (in Russian).
5. Minich R.W. et al. 1982, Phys.Lett., 118B, 458.
6. Gross D.H.E. et al. 1982, Z.Phys. A309, 42.
7. Friedman W.A. and Lynch W.G., 1983, Phys.Rev., C28, 950.
8. Randrup J. and Koonin S. 1981, Nucl.Phys. A356, 223.
9. Das Gupta S. and Mekjian A.Z. 1981, Phys.Rep., 72, 131.
10. Bondorf J.P. et al. 1985, Nucl.Phys. 443A, 321.
11. Bondorf J.P. et al. 1985, Nucl.Phys. 444A, 460.
12. Bondorf J.P. 1982, Nucl.Phys. 387A, 25c.
13. Fai G. and Randrup J. 1982, Nucl.Phys. 381A, 557.
14. Aichelin J. 1984, Phys.Rev. C30, 107.
15. Campi X. 1984, Phys.Lett. 142B, 8.
16. Aichelin J. and Hüfner J. 1984, Phys.Lett., 136B, 15.
17. Kaufman S.B. et al. 1976, Phys.Rev. C14, 1121.
18. Hirose A.S. et al. 1984, Phys.Rev. C29, 508.
19. Bannik B.P. et al. 1985, Z.Phys. 321A, 249.
20. Bannik B.P. et al. 1984, Pisma Zh.Eksp.Teor.Fiz. 39, 184 (in Russian); JETP Lett. 39, 219.
21. Vokalova A. et al. 1984, JINR Communication, Dubna P1-84-532.
22. Andreeva N.P. et al. 1986, JINR Preprint, Dubna P1-86-8.
23. Ameeva B.U. et al. 1986, Izvestiya AN SSSR, Seria Fiz. 11, 2103.
24. Barashenkov V.S. et al. 1983, JINR Preprint, Dubna P2-83-117.
25. El-Naghy A. 1981, Z.Phys. A 302, 261.
26. Heckmann H.H. et al. 1978 Phys.Rev. 17C, 1735.

Received by Publishing Department
on July 15, 1987.

Эль-Наги А. и др.
Фрагментация ядер ^{22}Ne в фотоэмульсии
при 4,1 ГэВ/с

E1-87-547

Изучено зарядовое распределение фрагментов ^{22}Ne , образующихся в столкновении с ядрами фотоэмульсии при импульсе 4,1 А ГэВ/с. Исследованы корреляционные соотношения между фрагментами снаряда, между ними и фрагментами мишени. Изменение зарядового выхода фрагментов имеет место при большой "жесткости" столкновения. Настоящий анализ противоречит теоретическим расчетам зарядового распределения на основе модели испускания из одного источника.

Работа выполнена в Лаборатории высоких энергий ОИЯИ.

Препринт Объединенного института ядерных исследований. Дубна 1987

El-Naghy A. et al.
Fragmentation of ^{22}Ne in Emulsion at 4.1 A GeV/c

E1-87-547

Charge distributions of projectile fragments produced in the interactions of ^{22}Ne beams with emulsion at 4.1 A GeV/c have been studied. Correlations between projectile and target fragments and among projectile fragments are presented. The change of charge yield distribution with the violence of the collision has been shown. The present analysis contradicts theoretical calculations describing the inclusive charge yield distribution of fragments by a single process.

The investigation has been performed at the Laboratory of High Energies, JINR.

Preprint of the Joint Institute for Nuclear Research. Dubna 1987